Desalination and Water Treatment
www.deswater.com

26 (2011) 226–235
February

1944-3994/1944-3986 © 2011 Desalination Publications. All rights reserved
doi: 10/5004/dwt.2011.1502

Mass and heat transport resistance in pervaporation process

Andrzej Noworyta*, Monika Kubasiewicz-Ponitka, Antoni Koziol

Department of Chemistry, Wroclaw University of Technology, 50-370 Wybrzeze Wyspianskiego 27, Wroclaw, Poland
Tel. +48 71 3202653; email: andrzej.noworyta@pwr.wroc.pl

Received 22 April 2008; Accepted 1 September 2010

ABSTRACT

Using a solution-diffusion mechanism, the rate of mass transport in pervaporation process was determined. A method to determine the parameters of the applied model, i.e., mass transport coefficients in the liquid and gas phase and partition coefficients on both sides of membrane surface was presented. Experiments were conducted in phenol-water and p-cresol-water system using a PDMS composite membrane (Pervatech, the Netherlands). Results of vacuum pervaporation were used to calculate mass transfer resistance in the liquid phase and the partition coefficient on the membrane surface. Experimental values obtained in vacuum pervaporation have shown that resistance in the liquid phase is in the range from 10 to 40% of the total resistance and cannot be neglected. The experiments with a sweep gas pervaporation process allowed to determine mass transport resistance in the inert phase, which appeared to be a limiting parameter of the mass transport rate.

Keywords: Vacuum pervaporation; Sweep gas pervaporation; Mass transport; Organic compound

1. Introduction

Pervaporation is one of the recently developed, still not fully explained and described membrane processes. Its selectivity depends first of all on the applied membrane. For this reason, most references dedicated to pervaporation deal with the membranes properties and selective mass transport through membranes [1–6]. The first pervaporation membranes, dense by nature, were relatively thick (100–1000 μm) which implies high resistance of mass transport by diffusion. In such a case, resistance of other stages of interfacial mass transport was neglected. The permeate flux obtained using these membranes is small, and sometimes even very small. A decrease of separating layer thickness which occurs in thin, composite pervaporation membranes remarkably increases the permeate flux [1,3,6]. In this case mass transport resistance in the membrane decreases to such a level that it stops being predominant and should not be identified with total mass transport resistance.

In this paper, a solution-diffusion mechanism of the process was assumed and mass transport was described using a model, which is classical for chemical engineering, the resistances-in-series-model with the application of activity difference as a driving force of the process [7,8].

An argument for selecting this model is that for diluted solutions which will be discussed in the paper, mass transport in the pervaporation process proceeds according to the concentration (activity) gradient, and the effect caused by concentration polarization is negligible [9–13].

This results from the fact that in the pervaporation process, the membrane was selected in such a way as to show preferential transport of components relative to the solvent. In this case there is no concentration of these components at the membrane surface, which is

*Corresponding author.

characteristic of the concentration polarization. The accumulation can occur only in the case of a solvent. However, its concentration in the retentate in cases discussed in the present paper exceeds 99% wt. Hence, with sufficient accuracy the kinetics of its transport to the membrane surface can be identified with the kinetics of pure solvent transport.

Two cases of generating driving force were analyzed: either keeping a sufficiently high vacuum on the permeate side, or transferring inert (sweep) gas through the permeate chamber.

Fig. 1 shows the concentration profiles in vacuum pervaporation characteristic for solution-diffusion mechanism of the process. The total mass transport resistance for a given component can be divided into two parts [7,8,14,15]:

- resistance in the liquid phase, determined by convection and diffusion,
- resistance in the membrane, determined by diffusion and phase equilibrium.

The description of this process, classical for chemical engineering, leads to the equation:

$$J_j = \frac{1}{\frac{1}{k_{l,j}} + \frac{1}{m_{1,j}\frac{D_{m,j}}{s_m}}} \bullet \left(c_{r,j} \bullet \gamma_{r,j} - \frac{c_{4,j} \bullet \gamma_{4,j} \bullet m_{2,j}}{m_{1,j}}\right) \tag{1}$$

where partition coefficients on the interfaces (Fig. 1) are given by the relations

$$m_{1,j} = \frac{c_{2,j} \bullet \gamma_{2,j}}{c_{1,j} \bullet \gamma_{1,j}}; \qquad m_{2,j} = \frac{c_{3,j} \bullet \gamma_{3,j}}{c_{4,j} \bullet \gamma_{4,j}} \tag{2}$$

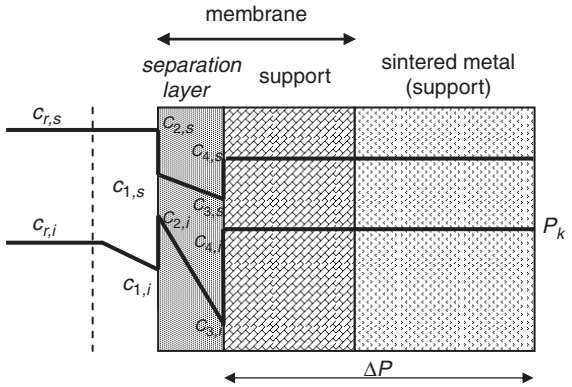

Fig. 1. Concentration profiles in vacuum pervaporation.

A further transport of mass, i.e., a mixture of the vapor of the system components from the dense membrane surface, proceeds by convection mechanism.

$$\sum P_{4,j}(c_{4,j}) = P_k + \Delta P = f \tag{3}$$

where f (support parameters, flow type, ΣJ_i)

Pressure drop in vapor transport trough both supports depends on their hydraulic parameters. Knowing these values one can define whether this is viscous or Knudsen flow, and after calculation of ΔP, the pressure ($P_{4,j}$) and its corresponding concentration of particular components ($c_{4,j}$) can be determined. The method to calculate pressure drop and values obtained for the applied equipment have been described earlier [16]. Next, from model Eqs. (1) and (2) mass flux and distribution of concentrations of components permeating through the membrane can be calculated. The parameters of this model are: $k_{1,j}$, $m_{1,j}$, $m_{2,j}$, $D_{m,j}$, s_m and P_k.

In the case of diluted solutions, the influence of cross effects on diffusion coefficient is small and can be considered insignificant in the discussed process [7,17]. Hence, it was assumed that the diffusion coefficient was constant [7,12].

Fig. 2 shows the concentration profiles in the case of sweep gas application. In this version of the process, the difference of concentrations is a driving force at all stages of mass transport. Mass flux is described by the equation

$$J_j = \frac{1}{\frac{1}{k_{l,j}} + \frac{1}{m_{1,j} \bullet \frac{D_{m,j}}{s_m}} + \frac{m_{2,j}}{m_{1,j} \bullet \varepsilon \bullet \frac{D_{g,j}}{s_s}} + \frac{m_{2,j}}{m_{1,j} \bullet \varepsilon \bullet k_{g,j}}} \bullet \left(c_{r,j} \bullet \gamma_{r,j} - \frac{c_{6,j} \bullet \gamma_{6,j} \bullet m_{2,j}}{m_{1,j}}\right) \tag{4}$$

The first two terms of the denominator are identical as in case of vacuum pervaporation and describe mass

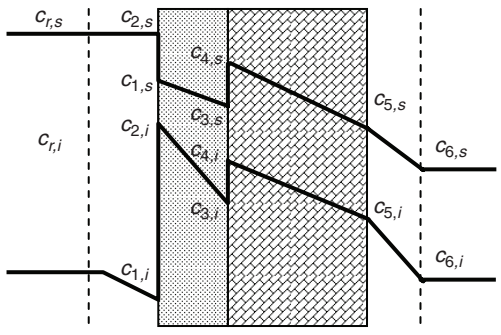

Fig. 2. Concentration profiles in sweep gas pervaporation.

transport resistance in the liquid phase and in the membrane separation layer. Two others terms of the denominator represent resistance of mass transport through the pervaporation membrane support and to the gas phase. It is worth noting that due to a porous structure of the membrane support, different from the structure of membrane separation layer, the area of surface through which mass is transported, is the other one. This is expressed by parameter ε porosity of membrane support (ε). The additional parameters of this model are: $D_{g,j}$, $k_{g,j}$, s_s, ε.

Mass transport in the pervaporation process is accompanied by heat transport [7,18]. Fig. 3 shows a temperature profile occurring in a sweep gas pervaporation. Heat required to evaporate the permeate stream is taken from the retentate stream.

In the case of vacuum pervaporation, assuming the process is adiabatic, the heat balance is described by the following equation

$$Q_r \bullet c_{p,r} \bullet (T_{r,in} - T_{r,out}) = \dot{Q}_1 = \Sigma J_j \bullet r_j \tag{5}$$

The following equation describes heat transport from retentate to the interface membrane separation layer and membrane support, where the stream of permeating components is evaporated:

$$\dot{Q}_1 = K_1 A \bullet (T_r - T_2) \tag{6}$$

where heat transfer coefficient (K_1) is expressed by the relation:

$$\frac{1}{K_1} = \frac{1}{\alpha_l} + \frac{s_m}{\lambda_m} \tag{7}$$

In the case of pervaporation to gas stream, there is an additional heat stream whose direction depends on the sign (+/–) of temperature difference in Eq. (8)

$$\dot{Q}_2 = K_2 \bullet A \bullet (T_2 - T_g) \tag{8}$$

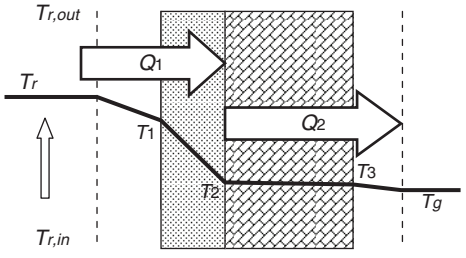

Fig. 3. Temperature profile in inert gas pervaporation.

where

$$\frac{1}{K_2} = \frac{1}{\varepsilon \bullet k_g} + \frac{s_s}{\varepsilon \bullet \lambda_s} \tag{9}$$

Heat flux used to the evaporation of permeate is the difference of $\dot{Q}_1$ and $\dot{Q}_2$.

2. Experimental

Experiments were carried out using a homogeneous water solutions of phenol (POCH Gliwice, Poland) and p-cresol (REACHIM, Poland) in a batch process at the concentration of 0.25–4.0 kg m^{-3}. A separating membrane was a commercial composite membrane with a dense polydimethylsiloxane film (2 μm) (PDMS) supported on a porous polyacrylonitrile carrier (PAN) (Pervatech, the Netherlands) with porosity 0.4. In vacuum pervaporation experiments were performed on a Sulzer Chemtech (Germany) laboratory system, where ca. 2 l of retentate circulated between the membrane module and feed tank (Fig. 4). In the experiments feed temperature was monitored in the tank, as well as at the inlet and outlet from the membrane cell. Pressure on the permeate side was reduced by a vacuum pump.

To carry out experiments with sweep-gas, a self-made pervaporation cell without a support from sintered metal was built. The membrane cell structure allowed us to maintain the same retentate hydrodynamics as in the vacuum pervaporation system. The membrane was supported on a grid made from steel bars of diameter 0.8 mm distant from each other by 10 mm. In the case of sweep gas pervaporation air was blown through the permeate zone in the membrane cell. Before entering the membrane cell, the air taken from atmosphere was heated up to decrease its relative humidity. Similar to the vacuum pervaporation the process was carried out in batch system.

In both analyzed pervaporation systems, permeate vapors entered a two-section system of condensers that operate alternatively. That made possible to take the collected permeate to analysis without disturbing the process. A cooling medium was a mixture of ice with calcium chloride at the temperature 261K.

To determine the permeate stream, condensed vapors were heated up to room temperature and then weighed. Streams of particular permeates were calculated from the total mass flux and organic substance concentration in the permeate. Each time, during the experiment the retentate composition was also measured.

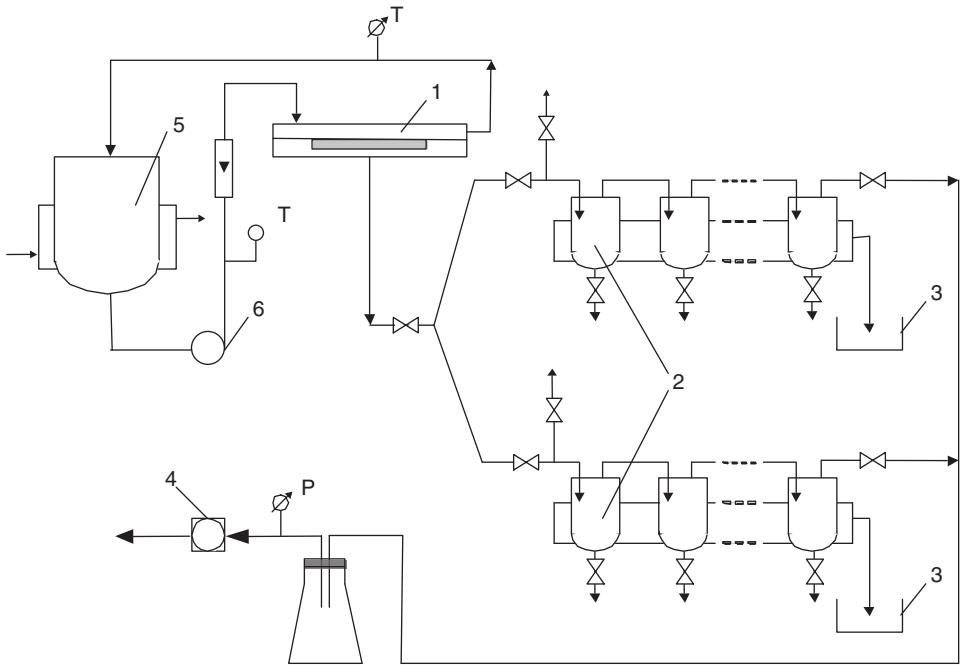

Fig. 4. Experimental setup: 1-membrane cell, 2-cold traps, 3-tank of molten refrigerant, 4-vacuum pump, 5-buffer tank, 6-feed pump.

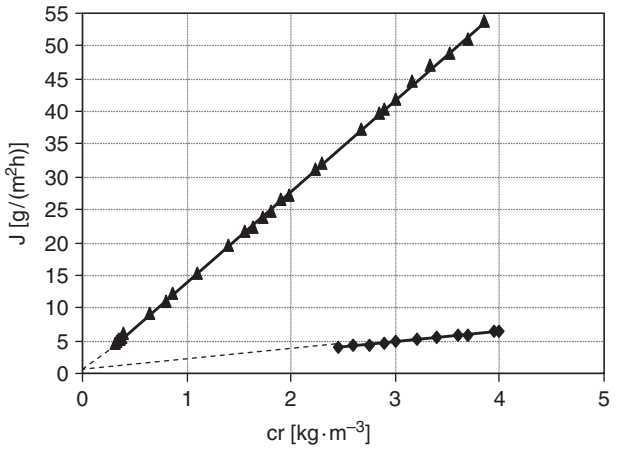

Fig. 5a. Phenol stream vs. its concentration in retentate at T = 333 K: ▲ in vacuum pervaporation (P_k<1 hPa), ◆ in sweep gas pervaporation (Q_g = 6.910^{-5} m^3 s^{-1}).

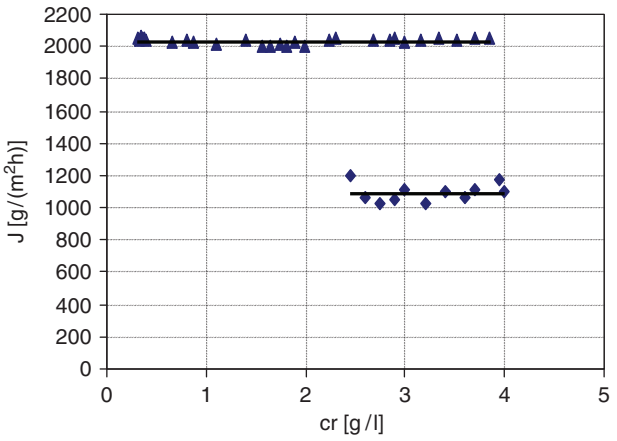

Fig. 5b. Water stream vs. phenol concentration in retentate at T = 333 K: ▲ in vacuum pervaporation (P_k<1 hPa), ◆ in sweep gas pervaporation (Q_g = 6.910^{-5} m^3 s^{-1}).

3. Results and discussion

The series of experiments were carried out for different retentate flow and concentration, temperature and pressure in the condensation zone. Examples of values characterizing the process are given in Figs. 5a and 5b.

3.1. Determination of parameters in the model

Since pervaporation is not an isothermal process, first for each experiment a temperature gradient along mass transport way was calculated. Basing on the knowledge of the permeate stream and its composition, heat flux required to permeate evaporation was calculated. For permeate streams obtained at retentate temperature ranging from T_r = 323–353 K, this value was Q = 16–47 W, respectively. Using the heat balance equation (Eq. [5]) a decrease of retentate temperature at the flow through a pervaporation cell was calculated. In vacuum pervaporation, where permeate streams and also heat fluxes were the much biggest then sweep gas pervaporation,

temperature drop on the retentate did not exceed 0.1 K. Hence, it can be concluded that in the cell on the retentate side the conditions are isothermal. This was confirmed experimentally by measuring a temperature difference in the retentate at the membrane cell inlet and outlet.

To estimate the coefficient of heat transfer from the retentate to membrane surface, a number of correlations for heat transfer to a flat wall were analyzed and the following one was selected [1,11].

$$\mathrm{Nu} = 0.66 \cdot \mathrm{Re}^{0.5} \cdot \mathrm{Pr}^{0.33} \tag{10}$$

In this equation a characteristic linear dimension to calculate the Nusselt and Reynolds numbers is the length of plate L. It was assumed that L was equal to the membrane cell radius. The equation holds when Re < 400,000 and Pr > 0.6.

Experiments carried out at varying process parameters showed that water was a dominating component of the permeate, and its stream depended only on temperature (Fig. 5b). As a result, a change of the retentate stream has practically no influence on heat flux needed for evaporation ($\dot{Q}_1$). Heat transport coefficient which influences the membrane surface temperature (T_1) depends on the retentate flow turbulence. The value of transfer coefficient in the applied retentate stream $Q_r = 2.03 \times 10^{-5}$ to 9.37×10^{-5} [m^3 s^{-1}] and temperature T_r = 323–353 [K] ranged from α_l = 441–1012 [W m^{-2}K^{-1}]. Fig. 6 shows the dependence of temperature difference T_r and T_1, calculated on this base on the retentate stream.

This is a significant temperature drop which should not be neglected, particularly for partition coefficient determination.

Temperature T_2 was calculated at the known thermal conductivity coefficient which was $\lambda_m = 0.185$ [W m^{-1}K^{-1}] for polydimethylsiloxane [2]. The value of T_2 is practically equal to T_1, which means that there is no temperature gradient in the membrane separation layer.

In the determination of partition coefficient $m_1(T_2)$ by means of subsequent approximations, the calculated temperature profile in each experiment was taken into account.

In the case of pervaporation to sweep gas, it was found that heat flux $\dot{Q}_2$ between the dense membrane surface and air stream could totally be neglected, and the temperature profile in this part of the system has no effect on the process.

In a previous paper pressure drop during flow through the membrane supports and the effect of pressure in the condensation zone on the permeate stream was analyzed [16]. For the small values of pressure P_k a linear decrease of the stream was observed with an increase of this pressure. In this paper values of permeate stream obtained at pressure P_k extrapolated to zero were taken to calculation.

In order to determine mass transport coefficient in the liquid phase in the vacuum pervaporation system, permeate streams were measured at different values of a retentate stream. Fig. 7 shows an example of the relation.

It is assumed that mass transfer coefficient in the liquid phase can be described by the correlation [11,12,19]

$$\mathrm{Sh} = C \cdot \mathrm{Re}^{a} \cdot \mathrm{Sc}^{0.33} \tag{11}$$

The Reynolds number is defined as

$$\mathrm{Re} = \frac{w \cdot d_h \cdot \rho}{\eta} = \frac{Q \cdot d_h \cdot \rho}{A \cdot \eta} \Rightarrow \frac{Q \cdot \rho}{d_h \cdot \eta} \tag{12}$$

where d_h is the membrane cell radius (d_h = 0.07 m). Values of Reynolds number in the measurements range from 600 to 2800.

Using the experimentally determined dependence of the flux of a given component on its concentration in the retentate, model parameters were estimated by means of nonlinear regression. The regression analysis was performed for the equation which had been obtained

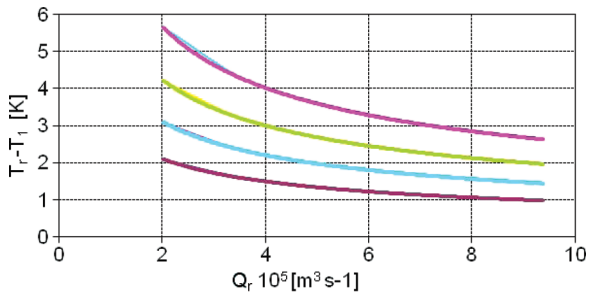

Fig. 6. Dependence of temperature drop in the near membrane layer on retentate stream (Q_r) and its temperature: ▲ 323 K, ◆ 333 K, ● 343 K, ■ 353 K.

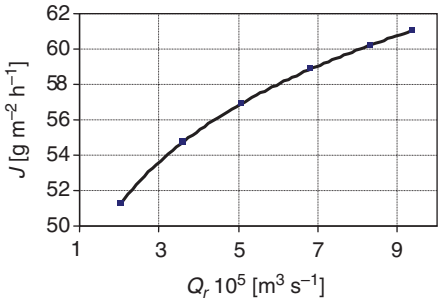

Fig. 7. Dependence of phenol stream on retentate stream for c_r = 4, 0 kg m^{-3}, T_r = 333 K, P_k = 0.

after substituting to Eq. (1) the value of mass transfer coefficient (k) described by Eq. (11).

In the first step of approximation, both two activity coefficients were assumed to be equal to unity.

Term $\frac{c_{4,j} \cdot \gamma_{4,j} \cdot m_{2,j}}{m_{1,j}}$ in model equation containing parameter m_2 appeared statistically insignificant in the regression analysis. This means that in the experimental conditions it can be assumed that driving force of the process is a function of concentration of a given component in the retentate.

$$c_{r,j} \cdot \gamma_{r,j} - \frac{c_{4,j} \cdot \gamma_{4,j} \cdot m_{2,j}}{m_{1,j}} \cong c_{r,j} \cdot \gamma_{r,j} \tag{13}$$

This simplification is justified because in a diluted solution which in the considered case is the retentate, the activity coefficient is usually much higher than unity, and then the subtracted term in Eq. (13) could be omitted. Hence, the model equation can be simplified to the form:

$$J_j = \frac{1}{\frac{1}{k_{l,j}} + \frac{1}{m_{1,j}\frac{D_{m,j}}{s_m}}} \cdot c_{r,j} \cdot \gamma_{r,j} \tag{14}$$

In final regression analysis the following equation was used:

$$J_j = \frac{1}{\frac{1}{k_{l,j} \cdot \gamma_{r,j}} + \frac{1}{m_{1,j} \cdot \gamma_{r,j}\frac{D_{m,j}}{s_m}}} \cdot c_{r,j} \tag{15}$$

The correctness of this equation was confirmed by experimental data presented in Fig. 5.

It was assumed that the value of activity coefficient is constant in the considered range of process parameters. This simplification leads to identical formulas which were obtained in the classical approach used in chemical engineering, where the difference of concentrations of a given component is used to determine k (e.g., Eq. [11]) and m.

$$J_j = k_j^* \cdot \Delta c_j \tag{16}$$

$$k_{l,j}^* = k_{l,j} \cdot \gamma_{r,j} \tag{17}$$

$$m_{1,j}^* = m_{1,j} \cdot \gamma_{r,j} \tag{18}$$

A result of the calculations are the values of $m_{1,j}^*$, C and a.

The obtained values constants in Eq. (11) were $C = 2.06$ and $a = 0.54$. Due to invariable geometric parameters of the used apparatus, the obtained correlation is valid only for the tested equipment. Exponent at the Reynolds number is close to values characteristic of similar mass transport cases [7,11]. The values of partition coefficients $m_{1,j}^*$ determined simultaneously for the tested substances depending on temperature are given in Table 1. The temperature gradient discussed above was taken into account in the calculations. For practical reasons the value of $m_{1,j}^*$ in Table 1 was referred to the retentate temperature.

Much lower values for water confirmed that the applied membrane was hydrophobic and the transfer of organic substances was privileged; for p-cresol being more hydrophobic than phenol, the partition coefficient is higher.

In sweep gas pervaporation, mass transport in the liquid phase and in the membrane separation layer proceeds in the same way as in the vacuum process. Using results of the experiments carried out at different air streams (Fig. 8), an attempt was made to estimate model (Eq. [4]) parameters, i.e., $k_{g,j}$ and $m_{2,j}$, applying nonlinear regression.

For this purpose it was assumed that mass transfer coefficient in the gas phase can be described by the correlation analogous (Eq. [11]) to that used in the case of transfer in the liquid phase. Due to a slightly

Table 1
Values of partition coefficient m_1^*

T [K]	Phenol	p-cresol	Water
323	0.178	0.811	$0.926 \cdot 10^{-4}$
333	0.275	1.185	$1.280 \cdot 10^{-4}$
343	0.460	1.690	$1.600 \cdot 10^{-4}$
353	0.650	2.425	$2.000 \cdot 10^{-4}$

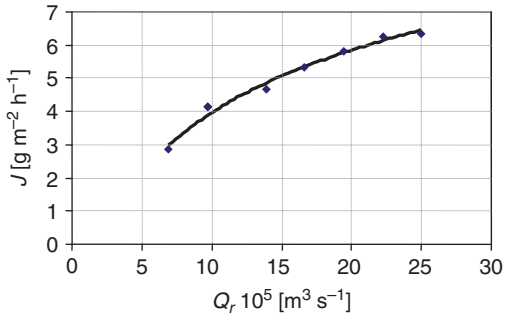

Fig. 8. Phenol stream vs. air stream for retentate temperature $T = 333$ K and concentration $c_r = 4.0$ kg m^{-3}.

Table 2
Values of $m_2 C^{-1}$

T [K]	Phenol	p-cresol	Water
323	97.1	21.1	$11.2 \cdot 10^4$
333	106.4	27.3	$14.1 \cdot 10^4$
343	111.1	37.2	$16.0 \cdot 10^4$
353	129.9	46.9	$21.2 \cdot 10^4$

different stream profile in the permeate chamber and a principally different range of the Reynolds number (60–215), the constants values of correlation obtained from the analysis of mass transport in the liquid phase cannot be used. The applied procedure was the same as in the case of vacuum pervaporation.

The statistical analysis shows that also in this case term $\frac{c_{6,j} \cdot \gamma_{6,j} \cdot m_{2,j}}{m_{1,j}}$ in model Eq. (4) and mass transport resistance in membrane support were insignificant. Consequently, on the basis of mentioned experiments constant C in correlation (11) and parameter $m_{2,j}$ could not be determined as separate values. It was only possible to calculate the resistance of mass transport to the gas phase (the fourth component of sum in the denominator of Eq. [4], and on this basis the exponent at the Reynolds number a = 0.66 and quotient $C/m_{2,j}$ were determined.

Values of this quotient given in Table 2 allow us to analyze the effect of temperature on partition coefficient $m_{2,j}$. In this case, just as it was with $m^*_{1,j}$, the values of this quotient were referred to the retentate temperature. It is worth noting that due to evidently smaller streams of mass than in the vacuum pervaporation, in the case of pervaporation to sweep gas the temperature gradient is much smaller.

A decrease of $m_{2,j}$ with temperature growth is observed. However, equilibrium in this case refers to the membrane-gas system and depends additionally on a given component saturation pressure.

4. Analysis of mass transport resistances

Fig. 9a–9c illustrate the temperature dependence of relative (in ratio to the values for T = 323 K) permeate fluxes, saturated vapor pressure and partition coefficient m_1 for phenol, p-cresol and water, respectively.

These values do not overlap. The saturated vapor pressure increases much faster than the permeate flux of a given component.

In many models of mass transport through the dense membrane described in literature [1,6,15,18], a driving force of the process is taken like the difference of saturated vapor pressure and partial pressure of a given substance on the permeate collection side, the latter being usually compared to zero. In this approach, the model would predict the obviously overestimated values of the permeate stream. Hence, to obtain model values corresponding to experimental ones, the other parameter of

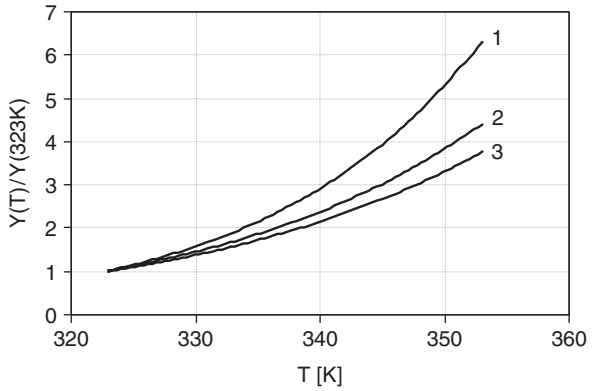

Fig. 9a. Dependence of relative saturated vapor pressure of phenol (1), its flux at retentate concentration c_r = 4.0 gl^{-1} (2) and m_1^*(3) on feed temperature.

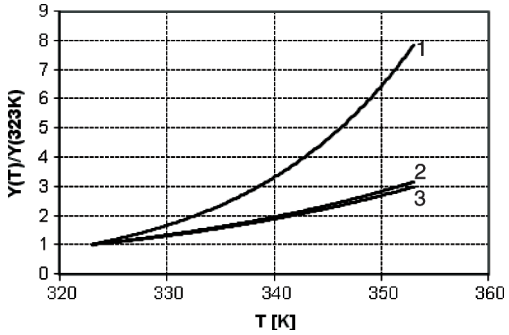

Fig. 9b. Dependence of relative saturated vapor pressure of p-cresol (1), its flux at retentate concentration c_r = 4.0 gl^{-1} (2) and m_1^*(3) on feed temperature.

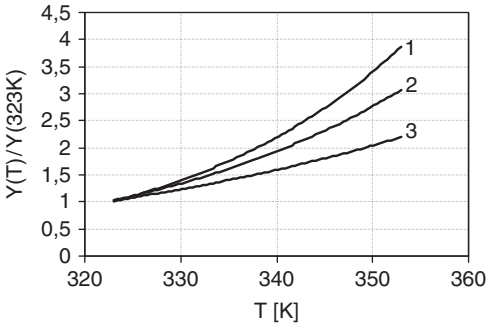

Fig. 9c. Dependence of relative saturated vapor pressure of water (1), its flux (2) and m_1^*(3) on feed temperature.

mentioned models, the so-called membrane permeability, which is expressed as a product of solubility and diffusivity of a substance penetrating the membrane should be a significant decreasing function of temperature. However, physicochemical measurements [4,9,18] do not confirm such a relation, which underrates these models.

The discussed model covers all stages of mass transport and the knowledge of model parameters enables determination of the contribution of their resistances. Table 3 gives values of diffusion coefficients in the membrane and air for substances tested in this study.

Table 4 gives values an example that characterize mass transport in the tested vacuum pervaporation system. Due to low concentration of substances dissolved in the retentate, mass transfer resistance of water in the liquid phase could be wholly neglected.

In the considered cases mass transport resistance in the liquid phase ranges from 10 to 40% and increases with process temperature growth. This follows from the fact that mass transfer coefficient in the liquid phase grows with temperature increase much slower than the partition coefficient m_1 and the coefficient of diffusion through the membrane. This resistance is significant and should be minimized by a proper structure of the retentate channel in membrane module and appropriate selection of retentate stream turbulence. The above remarks refer to pervaporation membranes with the thickness of some microns only. Earlier produced pervaporation membranes with separating layer thickness of 100–1000 μm generate linearly bigger resistance to diffusion, which in many cases makes this transport resistance through membrane equals total mass transport resistance. The results obtained allow us to determine absolute values of mass transfer coefficient in the liquid phase and to compare it with transport resistance through different membranes.

Table 5 shows a comparison of mass transport resistance for phenol-water system which is characteristic of sweep gas pervaporation. The resistance of transport by diffusion through the membrane support, as negligible, is not presented in the table.

A similar distribution of mass transport resistance was obtained for the p-cresol-water system. It follows from Table 5 that transport resistance in the gas phase is very high. It constitutes 80–90% of the total mass transfer resistance for organic substances and 37–48% for water. Hence, in the case of this pervaporation method, the conditions of mass transport in the gas phase should be intensified.

5. Selectivity of the process

The proposed model enables very simple analysis of process selectivity. The selectivity of the mentioned process is limited (Eq. [19]) to the ratio of total mass transfer coefficients k_{ov} for the compared components.

Table 3
Values of diffusion coefficient $m^2\ s^{-1}$

T [K]	Phenol		*p*-cresol		Water	
	Membrane	Air	Membrane	Air	Membrane	Air
323	$3.2\cdot10^{-11}$	$0.98\cdot10^{-5}$	$2.2\cdot10^{-11}$	$0.89\cdot10^{-5}$	$0.84\cdot10^{-8}$	$2.97\cdot10^{-5}$
333	$3.7\cdot10^{-11}$	$1.04\cdot10^{-5}$	$2.5\cdot10^{-11}$	$0.94\cdot10^{-5}$	$0.95\cdot10^{-8}$	$3.15\cdot10^{-5}$
343	$4.1\cdot10^{-11}$	$1.10\cdot10^{-5}$	$2.8\cdot10^{-11}$	$0.99\cdot10^{-5}$	$1.05\cdot10^{-8}$	$3.34\cdot10^{-5}$
353	$4.5\cdot10^{-11}$	$1.16\cdot10^{-5}$	$3.1\cdot10^{-11}$	$1.05\cdot10^{-5}$	$1.17\cdot10^{-8}$	$3.55\cdot10^{-5}$

Table 4
Mass transport coefficient in the liquid k_1^* and in the membrane $k_m=m_1^*D_{m,j}/s_m$, at retentate flow $Q_r = 9.39\cdot10^{-5}\ m^3\ s^{-1}$ and their contribution in total mass transfer resistance (R)

T [K]	Liquid phase						Membrane					
	Phenol		*p*-cresol		Water		Phenol		*p*-cresol		Water	
	$k_1^*\cdot10^5$ m s^{-1}	% R	$k_1^*\cdot10^5$ m s^{-1}	% R	k_l^* m s^{-1}	% R	$k_m^*\cdot10^6$ m s^{-1}	% R	$k_m^*\cdot10^5$ m s^{-1}	% R	$k_m^*\cdot10^6$ m s^{-1}	% R
323	2.39	10.7	2.21	18.0	∞	0	2.85	89.3	0.49	82.0	0.39	100
333	2.81	15.3	2.59	24.3	∞	0	5.09	84.7	0.83	75.7	0.61	100
343	3.24	22.4	2.99	31.1	∞	0	9.42	77.6	1.35	68.9	0.84	100
353	3.70	28.4	3.42	39.0	∞	0	14.6	71.6	2.18	61.0	1.17	100

Table 5
Mass transport coefficients (in 10^{-6} m s^{-1}) and distribution (in %) of mass transport resistance in sweep gas pervaporation for $Q_r = 1.81 \cdot 10^{-5}$ m^3 s^{-1} and $Q_g = 2.5 \cdot 10^{-4}$ m^3 s^{-1}

T [K]	Liquid phase				Membrane				Gas phase			
	Phenol		Water		Phenol		Water		Phenol		Water	
	k_l	%	k_l	%	k_m	%	k_m	%	k_g	%	k_g	%
323	9.81	2.7	∞	0	2.9	9.4	0.39	51.8	0.31	87.8	0.42	48.2
333	11.5	4.0	∞	0	5.1	9.0	0.61	52.1	0.52	87.1	0.66	47.9
343	13.3	6.0	∞	0	9.4	8.5	0.84	55.6	0.93	85.5	1.05	44.4
353	15.2	8.8	∞	0	14.7	9.0	1.18	62.5	1.61	82.2	1.96	37.5

$$S_{i/j} = \frac{\frac{c_{p,i}}{c_{p,j}}}{\frac{c_{r,i}}{c_{r,j}}} = \frac{\frac{J_i}{J_j}}{\frac{c_{r,i}}{c_{r,j}}} = \frac{\frac{J_i}{c_{r,i}}}{\frac{J_j}{c_{r,j}}} \cong \frac{k^*_{ov,i}}{k^*_{ov,j}} = \frac{1}{1/k^*_{l.i} + s_m / m^*_{1,i} \cdot D_{m,i}} \Big/ \frac{1}{1/k^*_{l,j} + s_m / m^*_{1,j} \cdot D_{m,j}} \tag{19}$$

where

$$S^m_{i/j} = \frac{m^*_{1,i} \cdot D_{m,i}}{m^*_{1,j} \cdot D_{m,j}} \tag{20}$$

is the membrane selectivity.

In the boundary case (a decay of mass transfer resistance in the liquid phase) the process selectivity is equal to membrane selectivity.

$$\lim_{k_l \to \infty} S_{i/j} = S^m_{i/j} \tag{21}$$

Fig. 10 shows examples of process selectivity obtained in the experiments. Selectivity of the used membrane calculated from Eq. (15) are 5,6; 7,8; 9,8 and 10,6 at temperatures 323, 333, 343 and 353 K, respectively.

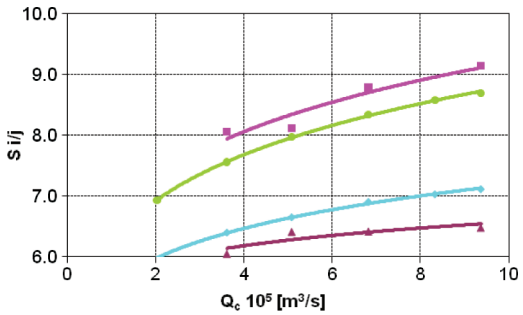

Fig. 10. The effect of retentate flow hydrodynamics on phenol separation coefficient at retentate concentration $c_r = 4$ kg m^{-3}, $P_k = 0$ and retentate temperature: ▲ 323 K, ◆ 333 K, ● 343 K, ■ 353 K.

6. Concluding remarks

Basing on results obtained in this work, the following conclusions can be drawn:

1. At the use of composite pervaporation membranes with thin separation layer mass transport resistance in the liquid phase (retentate) cannot be neglected. In our experimental conditions for organic substances it ranged from 10 to 40% of the total mass transport resistance.
2. Basing on the measurements of the permeate stream, partition coefficient at the liquid-membrane interface can be determined according to the method proposed in this paper. However, it is not possible to specify partition coefficient on the membrane-gas interface. When determining the value of m_1 one should take into account the temperature gradient resulting from heat transport.
3. In sweep gas pervaporation the biggest mass transport resistance occurs in the gas phase. In experimental conditions it composed 80–90% of the total mass transport resistance for organic substances and 37–48% for water. An intensification of mass transport conditions in this phase is the main objective in the sweep gas pervaporation method.

Acknowledgement

This work was supported by the project No. 343639/Z0311.

Symbols

A — surface, m^2
a — exponent (Eq. [11])
C — constant (Eq. [11])

C_p — heat capacity, J kg^{-1} K^{-1}
c — concentration, kg m^{-3}
D — diffusion coefficient, m^2 s^{-1}
J — pervaporation flux density, g m^{-2} h^{-1}
K — overall heat transfer coefficient, W m^{-2} K^{-1}
k — mass transfer coefficient, m s^{-1}
L — membrane cell radius, m
m_1, m_2 — partition coefficient on the membrane surface
P — pressure, Pa
P_k — pressure in the condensation zone, Pa
Q — volumetric stream, m^3 s^{-1}
$\dot{Q}$ — heat flux density, W m^{-2}
R — overall mass transport resistance, s m^{-1}
r — heat of vaporization, J kg^{-1}
S — selectivity
s — thickness, m
α — heat transfer coefficient, W m^{-2} K^{-1}
ε — porosity
λ — thermal conductivity, W m^{-1} K^{-1}
η — viscosity, kg m^{-1} s^{-1}

Subscripts

g — gas
i,j — component
l — liquid
m — membrane
p — permeate
r — retentate
s — support

$$\mathrm{N}u = \frac{\alpha \bullet L}{\lambda}$$

$$\mathrm{Pr} = \frac{\eta \bullet c_p}{\lambda}$$

$$\mathrm{Sh} = \frac{k \bullet L}{D}$$

References

[1] G. Mauviel, J. Berhiaud, C. Vallieres, D. Roizard and E. Favre, Dense membrane permeation: From the limitations of the permeability concept back to the solution-diffusion model, J. Membr. Sci., 266 (2005) 62–67.

[2] P. Wu, R.W. Field, R. England and B.J. Brisdon, A fundamental study of organofunctionalised PDMS membranes for the pervaporative recovery of phenolic compounds from aqueous streams, J. Membr. Sci., 190 (2001) 147–157.

[3] S. Han, L. Puech, R.V. Law, J.H.G. Steinke and A. Livingstone, Selection of elastomeric membranes for the separation of organic compounds in acidic media, J. Membr. Sci., 199 (2002) 1–11.

[4] M. Bennett, B.J. Brisdon, R. England and R.W. Field, Performance of PDMS and organofunctionalised PDMS membranes for the pervaporative recovery of organics from aqueous streams, J. Membr. Sci., 137 (1997) 63–88.

[5] E. Boscaini, M.L. Alexander, P. Prazeller and T.D. Mark, Investigation of fundamental physical properties of a polydimethylsiloxane PDMS membrane using a proton transfer reaction mass spectrometer (PTRMS), Int. J. Mass Spectrom., 239 (2004) 179–186.

[6] S.D. Doing, A.T. Boam, A.G. Livingstone and D.C. Stuckey, Mass transfer of hydrophobic solutes in solvent swollen silicone rubber membranes, J. Membr. Sci., 154 (1999) 127–140.

[7] R. Rautenbach and R. Albrecht, Membrane Processes, Chichester, John Wiley & Sons (1989).

[8] M. Mulder, Basic Principles of Membrane Technology, Kluwer Academic Publisher, Dordrecht.

[9] R. Jiraratananon, P. Sampranpiboon, D. Uttapap and R.Y.M. Huang, Pervaporation separation and mass transport of ethylbutanoate solution by polyether block amide (PEBA) membranes, J. Membr. Sci., 210 (2002) 389–409.

[10] A. Utriaga, D. Gorri and I. Ortiz, Mass–Transfer Modeling in the Pervaporation of VOCs from Diluted Solutions, AIChE J., 48(3) (2002) 572–580.

[11] V. Gekas and B. Hallström, Mass transfer in the membrane concentration polarization layer under turbulent cross flow I. Critical literature review and adaptation of existing Sherwood correlations to membrane operations, J. Membr. Sci., 30 (1987) 153–170.

[12] H.O.E. Karlsson and G. Trägårdh, Pervaporation of dilute organic–waters mixtures. A literature review on modelling studies and applications to aroma compound recovery, J. Membr. Sci., 76 (1993) 121–146.

[13] U. Beuscher and Ch.H. Gooding, The influence of the porous support layer of composite membranes on the separation of binary gas mixtures, J. Membr. Sci., 152 (1999) 99–116.

[14] L. Li, Z. Xiao, S. Tan, L. Pu and Z. Zhang, Composite PDMS membrane with high flux for the separation of organics from water by pervaporation, J. Membr. Sci., 243 (2004) 177–187.

[15] M. She and S.–T. Hwang, Concentration of dilute flavor compounds by pervaporation: Permeate pressure effect and boundary layer resistance modeling, J. Membr. Sci., 236 (2004) 193–202.

[16] A. Noworyta, M. Kubasiewicz–Ponitka and S. Mielczarski, An influence of support resistance on the pervaporation process efficiency, PERMEA 2005, In: The impact of membrane technology to human life, Electronics proceedings.

[17] R. Taylor and R. Krishna, Multicomponent Mass Transfer, New York, John Wiley (1993).

[18] E. Favre, Temperature polarization in pervaporation, Desalination, 154 (2003) 129–138.

[19] F.T. de Bruijn, L. Sun, Z. Olujic, P.J. Jansens and F. Kapteijn, Influence of the support layer on the flux limitation in pervaporation, J. Membr. Sci., 2232 (2003) 141–156.